

Hybrid Modeling (ML, Physical Model) for Prediction

Mounia El Arachi Amina Belemsaggam Wail Maghrane

January 8, 2024

Master Data Science

Supervision

- Pr. El Hassan Abdelwahed, Professor at the Faculty of Sciences Semlalia, Marrakech (FSSM) - Cadi Ayyad University.
- Phd. Oussama Hassidi at the Faculty of Sciences Semlalia

1 Introduction

Two different approaches have gained prominence in the field of predictive modeling. Predictive modeling is a dynamic statistical technique that uses machine learning and data mining to predict future outcomes by analyzing historical and existing data. Its versatility covers a variety of applications, from predicting TV viewership and customer behavior to assessing credit risk and corporate profits.

The essence of data-driven predictive modeling is to discover the relationships between system variables, both inputs and outputs, without an explicit understanding of the underlying physical characteristics of the system. This approach formulates predictive models based on existing data, predicting future outcomes by identifying patterns in the data set. Unlike models that rely on pre-selected variables, data-driven models are adaptive, continually revised and revised to reflect changes in the source data.

In the evolving landscape of machine learning and deep learning, applying these techniques to civil engineering challenges presents unique difficulties. Physics-based predictive modeling is a refined combination of machine learning with fundamental physical principles, including partial differential equations and mathe-

mathematical models. This approach alleviates challenges such as data misfit by incorporating the laws of physics into the training process, making it particularly relevant in disciplines such as fluid dynamics, quantum mechanics, and computational science.

In this context, physics-informed neural networks (PINNs) represent a state-of-the-art approach that seamlessly integrates machine learning with fundamental physical principles. This innovative methodology addresses the challenges associated with traditional machine learning applications in civil engineering and other scientific disciplines. PINNs use neural networks to solve inverse problems while respecting the laws of physics, making them applicable to scenarios where data may be limited or subject to drift. PINNs bridge the gap between data-driven and physics-driven approaches, offering a powerful predictive modeling tool across a variety of scientific disciplines.

In a practical context of application, froth flotation can play a key role in the mining industry. This widely used process can exploit differences in the surface properties of minerals to selectively separate valuable minerals from ores. In the context of PINN, the use of predictive modeling techniques can be crucial to optimize and understand the froth flotation process. PINNs can contribute by combining both data-driven knowledge and fundamental physics, ensuring accurate predictions and improved process efficiency.

2 Literature review

2.1 Data-driven and Physics-driven predictive modeling

2.1.1 What Is Predictive Modeling?

In short, predictive modeling is a statistical technique using machine learning and data mining to predict and forecast likely future outcomes with the aid of historical and existing data. It works by analyzing current and historical data and projecting what it learns on a model generated to forecast likely outcomes. Predictive modeling can be used to predict just about anything, from TV ratings and a customer's next purchase to credit risks and corporate earnings. A predictive model is not fixed; it is validated or revised regularly to incorporate changes in the underlying data. In other words, it's not a one-and-done prediction. Predictive models make assumptions based on what has happened in the past and what is happening now. If incoming, new data shows changes in what is happening now, the impact on the likely future outcome must be recalculated, too.

2.1.2 Data-Driven Predictive Modeling

The main aim of data-driven model concept is to find links between the state system variables (input and output) without clear knowledge of the physical attributes and behaviour of the system. The data driven predictive modelling derives the modelling method based on the set of existing data and entails a predictive methodology to forecast the future outcomes. It is data-driven only when there is no clear knowledge of the relationships among variables/system, though there is lot of data. Here, you are simply predicting the outcomes based on the data. The model is not based on hand-picked variables, but may contain unobserved, hidden combination of variables.

2.1.3 Physics-Driven Predictive Modeling

The recent development of machine learning (ML) and Deep Learning (DL) increases the opportunities in all the sectors. ML is a significant tool that can be applied across many disciplines, but its direct application to civil engineering problems can be challenging. ML for civil engineering applications that are simulated in the lab often fail in real-world tests. This is usually attributed to a data mismatch between the data used to train and test the ML model and the data it encounters in the real world, a phenomenon known as data shift. However, a physics-based ML model integrates data, partial differential equations (PDEs), and mathematical models to solve data shift problems. Physics-based ML models are trained to solve supervised learning tasks while respecting any given laws of physics described by general nonlinear equations. Physics-based ML, which takes center stage across many science disciplines, plays an important role in fluid dynamics, quantum mechanics, computational resources, and data storage.

2.2 Combination of AI and Physics

2.2.1 Combining AI and Physics?

Combining AI and Physics involves leveraging both machine learning techniques and domain-specific knowledge from physics to enhance the performance, accuracy, and interpretability of models. This integration can lead to more effective solutions, especially in scenarios where physical laws or principles govern the underlying processes.

2.3 Physics-informed neural network PINNs

Physics-Informed Neural Networks (PINNs) are a novel approach that integrates two methodologies: data-driven supervised learning via neural networks, and the

incorporation of physical equations to ensure the model’s consistency with the established physics of the system.

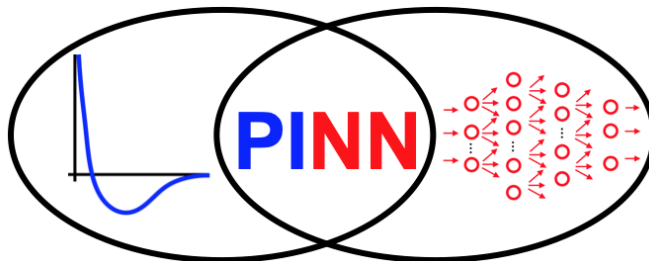


Figure 1: PINNs lie at the intersection between neural networks and physics

These physical equations are often expressed as Partial Differential Equations (PDEs). PINNs are particularly valuable in biological and engineering contexts where data scarcity can undermine the effectiveness of conventional machine learning techniques. Their robustness in low-data scenarios is a significant advantage.

Incorporating the principles of general physics into neural network training serves as a form of regularization. This regularization constrains the range of possible solutions, thereby enhancing the accuracy of the model’s approximations. By embedding this fundamental physical knowledge into a neural network, the effectiveness of the available data is amplified. This allows the learning algorithm to more accurately identify the correct solution and to generalize effectively, even when the quantity of training data is limited.

3 Our approach

3.1 Froth Flotation Overview :

Froth flotation is a widely employed process in the mining industry for the separation of valuable minerals from ores. Its success lies in exploiting the differences in the surface properties of minerals, allowing for selective attachment to air bubbles. The process is crucial for recovering economically valuable metals, such as zinc, iron, lead, and copper, from complex ore matrices.

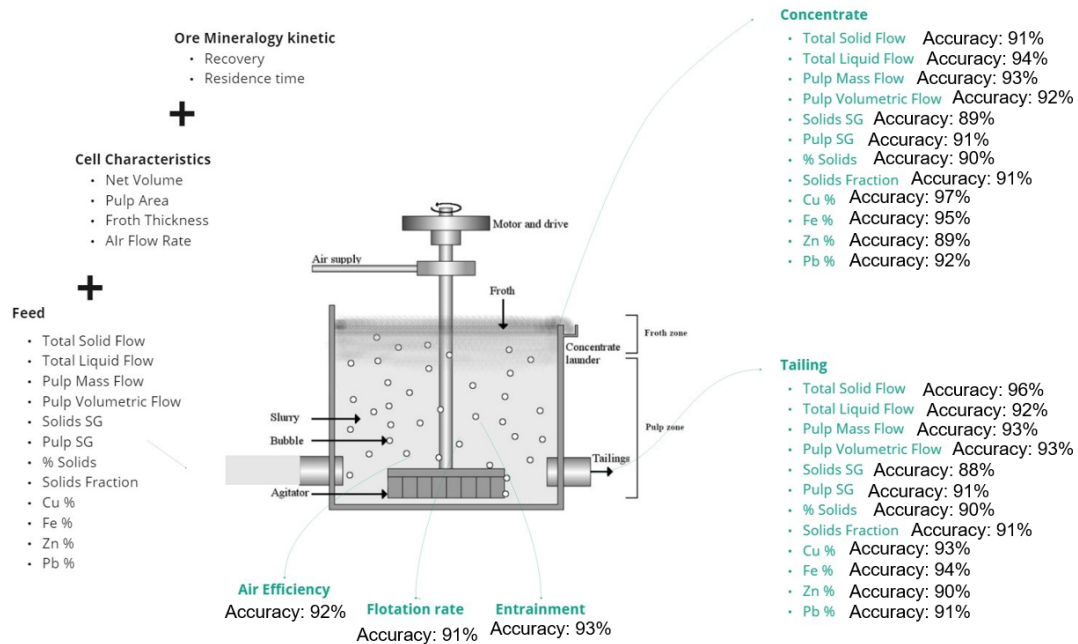


Figure 2: flotation cell

3.2 Key Stages of Froth Flotation:

3.2.1 Conditioning:

- Objective: Create a slurry with optimal hydrophobicity for selective mineral attachment.
- Process: Ore is ground into a fine powder and mixed with water, forming a slurry. Reagents, such as collectors and frothers, are added to modify the surface properties of minerals.

3.2.2 Aeration:

- Objective: Generate air bubbles that selectively attach to hydrophobic mineral particles.
- Process: The conditioned slurry is aerated by introducing air. The hydrophobic minerals selectively attach to the air bubbles, forming a froth layer on the liquid surface.

3.2.3 Separation:

- Objective: Separate the froth, carrying valuable minerals, from the pulp containing unwanted gangue minerals.
- Process: The froth is mechanically removed, and the remaining pulp, known as tailings, contains minerals that did not selectively attach to bubbles.

3.3 Physics-Informed Neural Networks (PINNs) in Froth Flotation:

3.3.1 AI in Froth Flotation:

- Objective: Enhance the accuracy of predictive models for froth flotation.
- Role: Artificial Intelligence (AI), particularly neural networks, is employed to capture complex non-linear relationships and patterns in the data, improving the understanding and prediction of flotation outcomes.

3.3.2 Physics-Informed Neural Networks (PINNs):

- Objective: Integrate physics-based constraints to enhance the physical consistency of predictions.
- Role: PINNs combine traditional neural networks with equations to ensure that the model adheres to fundamental physical laws governing the system.
- Equations :

Physical law	Equation	Reference
Conservation of mass	$\frac{dM_i}{dt} = m_{i,feed} - m_{i,tailings} - m_{i,TF} - m_{i,ENT}$	Minerals Engineering
Air flowrate of each bubble size class	$Q_{air,in}^k = Q_{air,in} \Psi_{d_b,pulp}^k$	Minerals Engineering
Flowrate out of the flotation tank	$Q_{pulp,out} = Q_{tailings} + Q_{conc}$	Minerals Engineering
Tailings particle concentration	$C_{i,tailings} = \frac{M_i}{V_{pulp}}$	Minerals Engineering
Gas volume of each bubble size class	$V_k^{gas} = \frac{\varepsilon_k^0}{1-\varepsilon_k^0} h_0 A_{cell}$	Minerals Engineering
Solid mass flowrate in the feed	$m_{i,feed} = C_{i,f} Q_{feed}$	Quintanilla et al., 2021
Pulp height	$h_p = \frac{h_0}{1-\varepsilon_{0,total}}$	Minerals Engineering
Pulp volume (liquid + gas)	$V_{pulp} = h_0 A_{cell} + V_{gas}$	Minerals Engineering

Table 1: some equations :

3.3.3 Integration of PINNs in Froth Flotation:

1. Differential Equation for Mass Conservation:

In the context of froth flotation or any dynamic process involving the movement and transformation of mass, the equation for mass conservation is a fundamental representation of the principle that mass is neither created nor destroyed. The chosen equation is a first-order linear differential equation, which is a simplified form representing the rate of change of mass with respect to time. The specific equation chosen for mass conservation in the given context is:

$$\frac{dM_i}{dt} = M_{i, feed} - M_{i, tailings} - M_{i, concentrate}$$

Here's an explanation of the components:

- dM/dt : This represents the rate of change of total mass (M) with respect to time (t). In other words, it describes how the total mass is changing over time.
- $M_{i,feed}$: The mass of mineral i in the feed.
- $M_{i,tailings}$: The mass of mineral i in the tailings.

- $M_{i, \text{concentrate}}$: The mass of mineral i in the concentrate.

This equation represents the change in the mass of mineral i over time, taking into account the inflow in the feed and outflows in the tailings and concentrate. The goal is to integrate this equation into the training of the neural network as part of the physics-informed regularization to ensure that the model adheres to the law of mass conservation. Here are the equations for each mineral :

$$\begin{aligned}\frac{dM_{\text{Zn}}}{dt} &= M_{\text{Zn, feed}} - M_{\text{Zn, tailings}} - M_{\text{Zn, concentrate}} \\ \frac{dM_{\text{Fe}}}{dt} &= M_{\text{Fe, feed}} - M_{\text{Fe, tailings}} - M_{\text{Fe, concentrate}} \\ \frac{dM_{\text{Pb}}}{dt} &= M_{\text{Pb, feed}} - M_{\text{Pb, tailings}} - M_{\text{Pb, concentrate}} \\ \frac{dM_{\text{Cu}}}{dt} &= M_{\text{Cu, feed}} - M_{\text{Cu, tailings}} - M_{\text{Cu, concentrate}}\end{aligned}$$

2. Equations in steady states : In steady state, the rates of change are zero, and the minerals are in balance between the feed, tails, and concentrate. These equations represent the steady-state conditions for the mass of each mineral in the concentrate.

$$\begin{aligned}M_{\text{Zn, feed}} &= M_{\text{Zn, tailings}} + M_{\text{Zn, concentrate}} \\ M_{\text{Fe, feed}} &= M_{\text{Fe, tailings}} + M_{\text{Fe, concentrate}} \\ M_{\text{Pb, feed}} &= M_{\text{Pb, tailings}} + M_{\text{Pb, concentrate}} \\ M_{\text{Cu, feed}} &= M_{\text{Cu, tailings}} + M_{\text{Cu, concentrate}}\end{aligned}$$

3. Physical Constraint (Loss Component): Enforces adherence to the equation representing mass conservation.

$$\begin{aligned}L_{\text{physics, Zn}} &= (M_{\text{Zn, feed}} - (M_{\text{Zn, tailings}} + M_{\text{Zn, concentrate}}))^2 \\ L_{\text{physics, Fe}} &= (M_{\text{Fe, feed}} - (M_{\text{Fe, tailings}} + M_{\text{Fe, concentrate}}))^2 \\ L_{\text{physics, Pb}} &= (M_{\text{Pb, feed}} - (M_{\text{Pb, tailings}} + M_{\text{Pb, concentrate}}))^2 \\ L_{\text{physics, Cu}} &= (M_{\text{Cu, feed}} - (M_{\text{Cu, tailings}} + M_{\text{Cu, concentrate}}))^2\end{aligned}$$

4. Prediction Loss :

The Prediction Loss is a component of the total loss function that assesses how well the neural network (NN) predictions match the actual or target values for each mineral. It quantifies the difference between the predicted values from the neural network and the observed values from the dataset. Here's a breakdown for each mineral:

$$L_{\text{prediction, Zn}} = \sum_{i=1}^N (Y_{Zn,i} - \text{NN}_{\text{Zn}}(X_i))^2$$

$$L_{\text{prediction, Fe}} = \sum_{i=1}^N (Y_{Fe,i} - \text{NN}_{\text{Fe}}(X_i))^2$$

$$L_{\text{prediction, Pb}} = \sum_{i=1}^N (Y_{Pb,i} - \text{NN}_{\text{Pb}}(X_i))^2$$

$$L_{\text{prediction, Cu}} = \sum_{i=1}^N (Y_{Cu,i} - \text{NN}_{\text{Cu}}(X_i))^2$$

5. Total Loss Function

Balances prediction accuracy and adherence to physics using a regularization parameter.

$$L_{\text{total}} = \lambda_{\text{physics}} \cdot \sum_i L_{\text{physics},i} + \lambda_{\text{prediction}} \cdot \sum_i L_{\text{prediction},i}$$

4 Development and Application

4.1 Architecture of Physics-informed Neural Network

The input data used by the ANN to predict or optimize the output data, which represents key performance indicators of a process, possibly in a mining or mineral processing context given the specific elements mentioned (Cu, Fe, Pb, Zn). The neural network architecture consists of five layers with a varying number of neurons in each layer, employing 'relu' activation functions in the hidden layers and a 'linear' activation function in the output layer.

Structure's parameters	ANN
Number of Layers	5
Number of neurons in the input layer	128
Number of neurons in the 1 st hidden layer	256
Number of neurons in the 2 nd hidden layer	512
Number of neurons in the 3 rd hidden layer	1024
Number of neurons in the output layer	10
Activation function of the input hidden layer	Relu
Activation function of the hidden layers	Relu
Activation function of the output layer	linear

Table 2: Structure's parameters for ANN

Input Columns
Net Volume
Pulp Area
Froth surface area
Froth thickness
Air Flow rate
R _{inf} C _{cp}
R _{inf} G _n
R _{inf} P _o
R _{inf} S _p
k _{max} C _{cp}
k _{max} G _n
k _{max} P _o
k _{max} S _p
Entrainment Savassi parameters
Total Solids Flow_Feed
Total Liquid Flow_Feed
Pulp Volumetric Flow_Feed
Solids SG_Feed
Pulp SG_Feed
Solids Fraction_Feed
Cu_Feed
Fe_Feed
Pb_Feed
Zn_Feed

Figure 3: Input Columns

Output Columns
Total Solids Flow_Concentrate
Total Solids Flow_Tailings
Cu_Tails
Fe_Tails
Pb_Tails
Zn_Tails
Cu_Concentrate
Fe_Concentrate
Pb_Concentrate
Zn_Concentrate

Figure 4: Output Columns

4.2 Training

The loss function is composed of lambda values: λ_{physics} and λ_{predict} , both weighted equally with a coefficient of 0.5. This hybrid approach ensures that the model’s predictions not only fit the observed data but also adhere to the underlying physical laws.

Initially, we utilized the ‘tanh’ activation function throughout the network. However, this choice resulted in suboptimal performance, indicating that ‘tanh’ was not capturing the complexities of our dataset. In response, we transitioned to using the ‘relu’ activation function, which led to a significant improvement in the model’s results. Subsequently, we increased the training regimen to a substantial 500 epochs to thoroughly train the model.

The loss components — `loss_predict` and `loss_physics` — are amalgamated to form the total loss function that drives the model’s learning process. This composite loss function has been instrumental in the model’s ability to generalize from the training data while remaining physically consistent.

A learning rate of 0.01 was selected as it provided a balanced pace for the model’s convergence during training. To enhance the training process further, we implemented checkpointing mechanisms. These checkpoints are strategic, as they allow us to save the model weights that yield the best performance at each epoch, which is particularly useful for long training sessions.

To quantify the model’s performance, we employed the R-squared (R^2) metric. The R^2 metric is a statistical measure that represents the proportion of variance for the dependent variable that’s explained by the independent variables in the model. This metric is particularly useful in gauging the model’s predictive power and its ability to capture the variance in the data.

Optimizer	Adam
Learning rate	0.01
Lambda physics	0.5
Lambda prediction	0.5
Loss function	Total Loss
Number of epochs	500

Table 3: PINN Parameters

5 Results

In this section, comprehensive visualizations are presented, offering a detailed comparison between the predictions generated by the Physics-Informed Neural Network (PINN) and the ground truth observed values for not only the total solids flow but also the concentrations of each individual mineral, namely Zinc (Zn), Iron (Fe), Lead (Pb), and Copper (Cu).

These visualizations aim to provide an in-depth understanding of the model's performance by elucidating its ability to accurately capture the intricate dynamics of both the overall mass flow and the specific compositional variations within the system.

5.1 Loss graphs

- The Train Loss and Validation Loss:

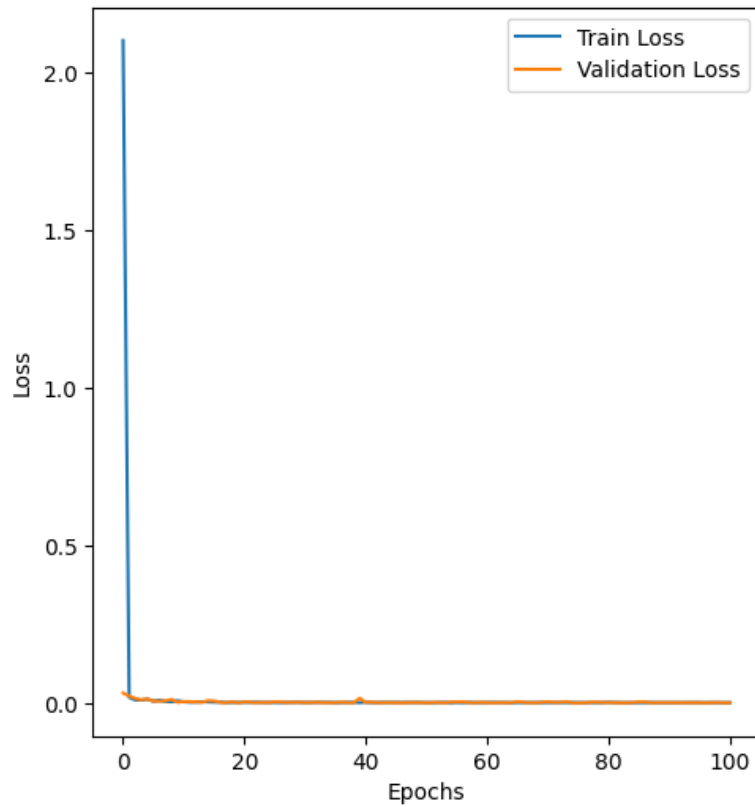


Figure 5: Train Loss VS Validation Loss

Description:

- Train Loss represents the loss measured on the training dataset during the training process. It shows a very sharp decrease at the beginning, dropping quickly to a value close to 0, which suggests that the model rapidly learned the training dataset.
- the validation loss, which is measured on a separate dataset not used during training. The validation loss provides an indication of how well the model can generalize to new data. In this graph, the validation loss also decreases sharply and remains close to the training loss throughout the training process.

This graph reflects a model that seems to have trained successfully, with no signs of overfitting or underfitting, assuming that the validation dataset is representative of the real-world data it will encounter.

- The R2 (R-squared) metric:

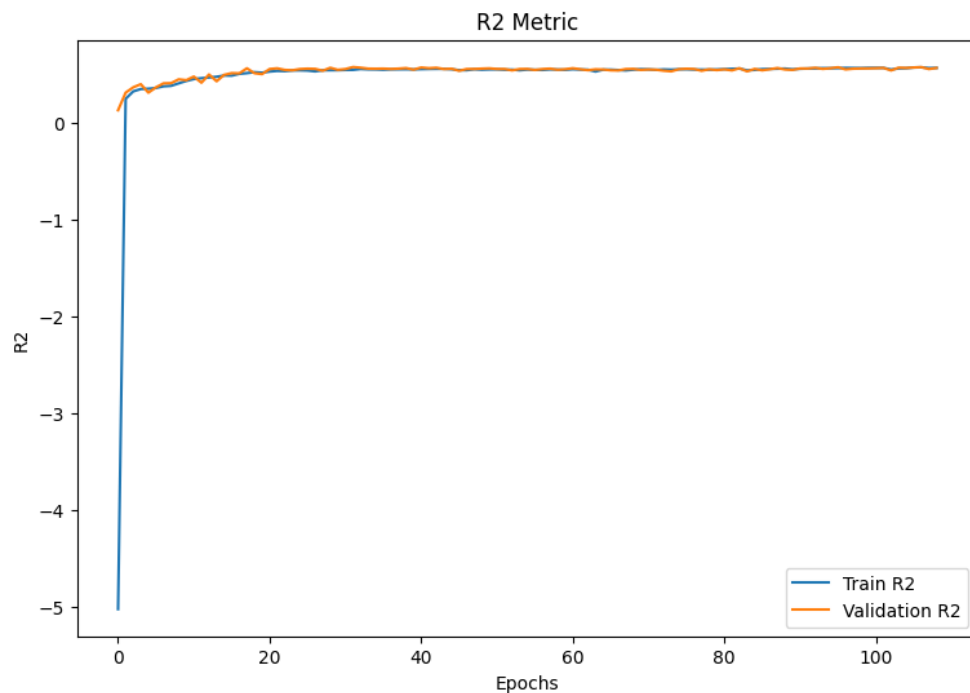


Figure 6: R2 (R-squared) Train VS R2 (R-squared) Validation

Description:

From the graph you provided, it appears that:

- The R^2 values for both training and validation data sets are converging to a value slightly below 0.5.
- The training R^2 starts from a negative value and quickly rises, whereas the validation R^2 starts from a higher value and slightly decreases before both lines flatten out.

5.2 Comparison of PINN Predictions with Actual Values of the total solids flow.

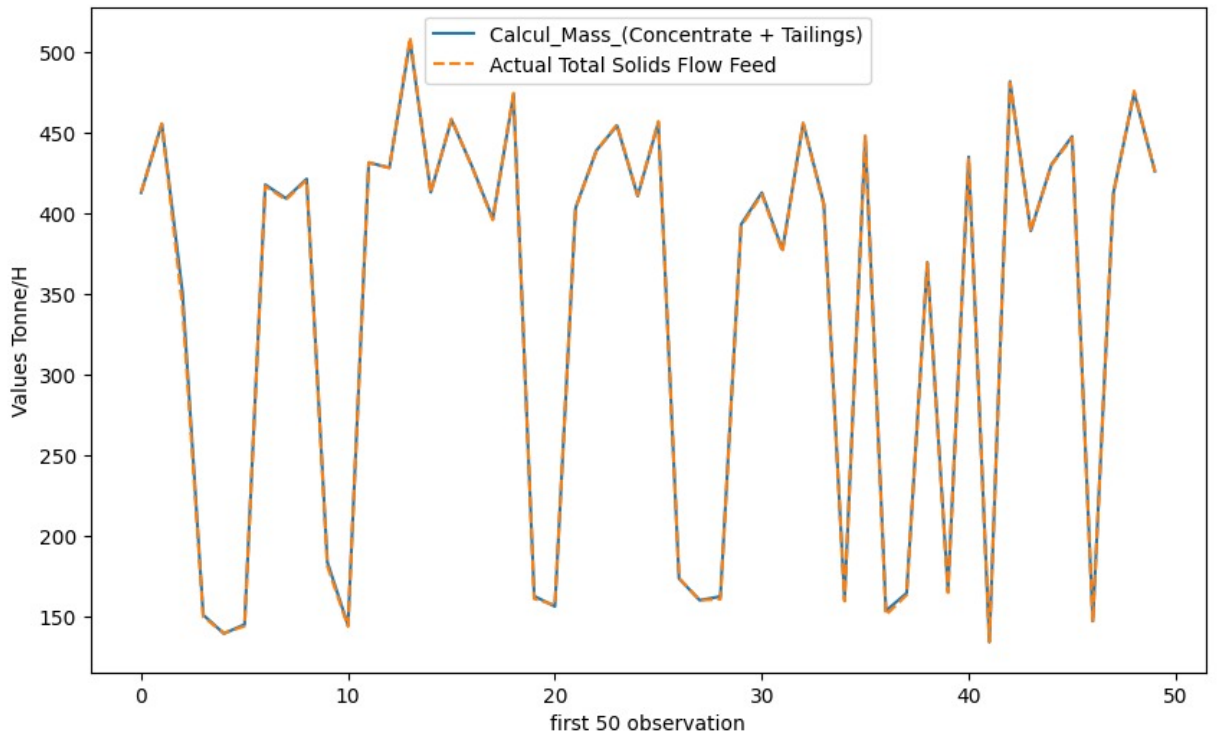


Figure 7: predicted sum (concentrate + tailings) VS actual total solids flow feed

Description

- **Calcul_Mass (Concentrate + Tailings) (solid blue line):** This line starts at a high point, drops to a lower value, then goes back up again, repeating this pattern over the 50 observations.

- **Actual Total Solids Flow Feed (dashed orange line):** It follows the same pattern as the *Calcul_Mass* line, with its high and low points occurring at the same times as the *Calcul_Mass* line.
- Both lines look very similar, rising and falling at the same points along the graph, which suggests that the calculated mass and the actual flow feed measurements match closely throughout the 50 observations. The lines do not separate much at any point, indicating that the values for each observation are almost the same for both the calculated mass and the actual flow feed.

5.3 Comparison of PINN Predictions with Actual Values of Zinc (Zn), Iron (Fe), Lead (Pb), and Copper (Cu) Concentrations.

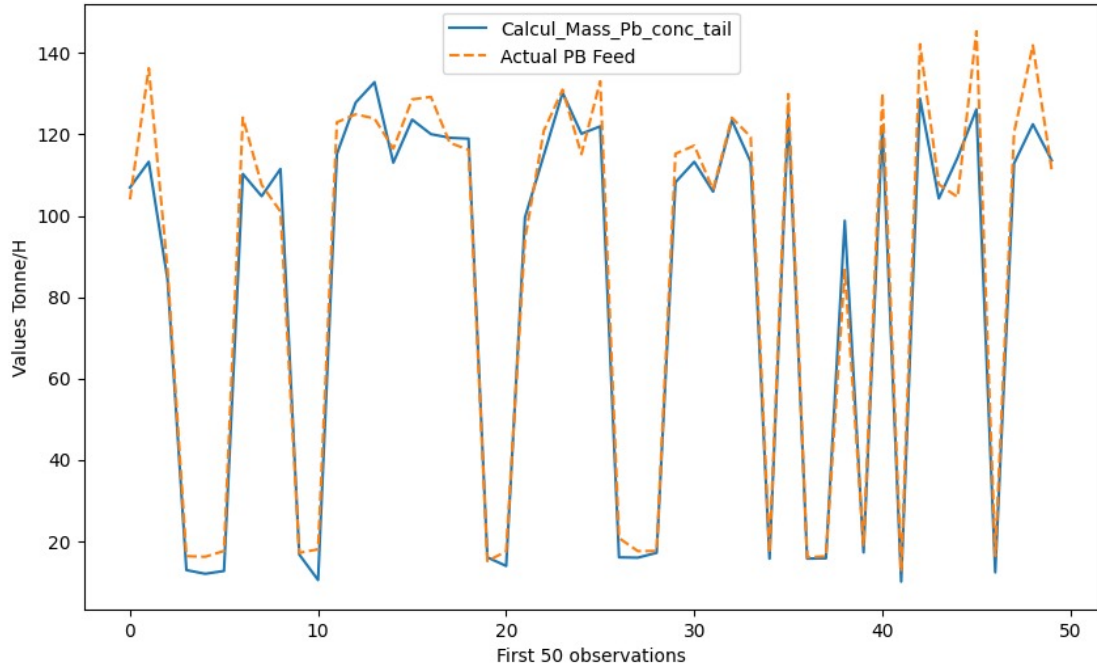


Figure 8: Predicted PB feed VS Actual PB feed

Description:

Calcul_Mass_Pb_conc_tail (solid blue line): It starts around 120 tonnes per hour, drops to about 40 tonnes per hour, then rises back up, and this pattern repeats through the graph.

Actual PB Feed (dashed orange line): This line goes up and down in a similar way to the *Calcul_Mass_Pb_conc_tail* line, indicating that the actual feed

of lead and the calculated mass of lead in the concentrate and tailings have similar values at each observation.

Both lines have the same general pattern, with their highest and lowest points appearing at the same time. This suggests that the two sets of measurements - the actual feed and the calculated mass - are very similar over the 50 observations.

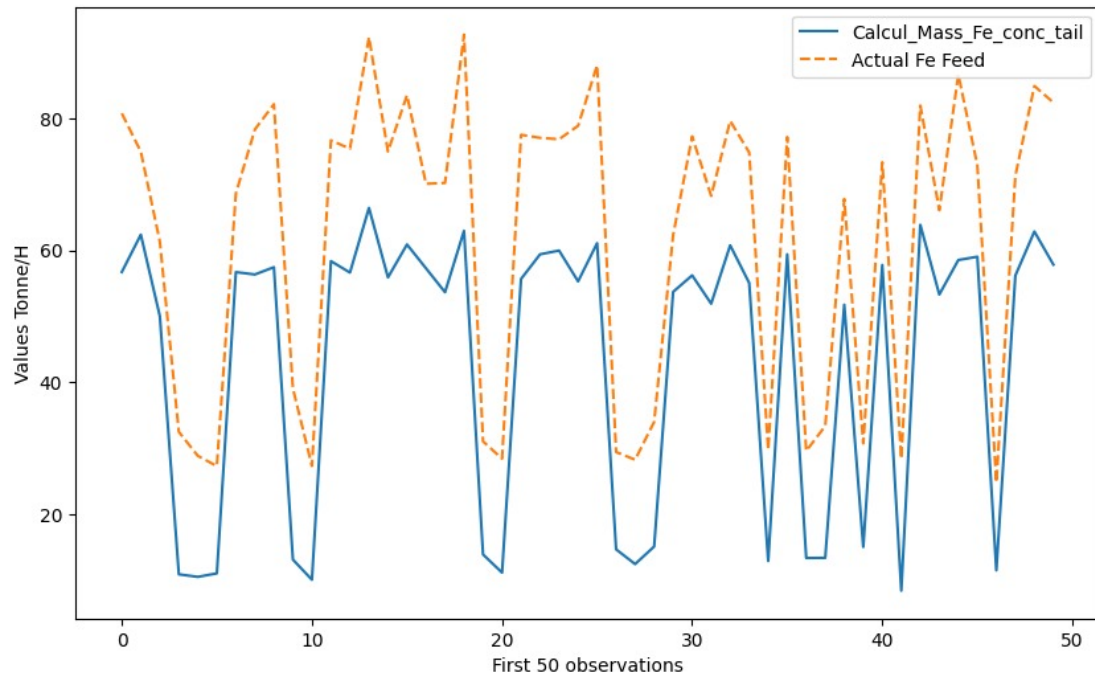


Figure 9: Predicted Fe feed VS Actual Fe feed

Description:

“Calcul_Mass_Fe_conc_tail (solid blue line):” This line goes up and down across the graph. It starts just above 60 tonnes per hour, drops sharply to around 20 tonnes per hour, rises back up to around 80 tonnes per hour, and continues this pattern.

“Actual Fe Feed (dashed orange line):” This line moves up and down in the same places as the *Calcul_Mass_Fe_conc_tail* line, indicating that the measurements for the actual feed and the calculated mass are close to each other at each point.

Both lines have a similar shape and pattern, which suggests that the calculated mass and the actual feed measurements behave similarly throughout the observations. They reach their high and low points at the same time, showing that they have similar measurements for each observation.

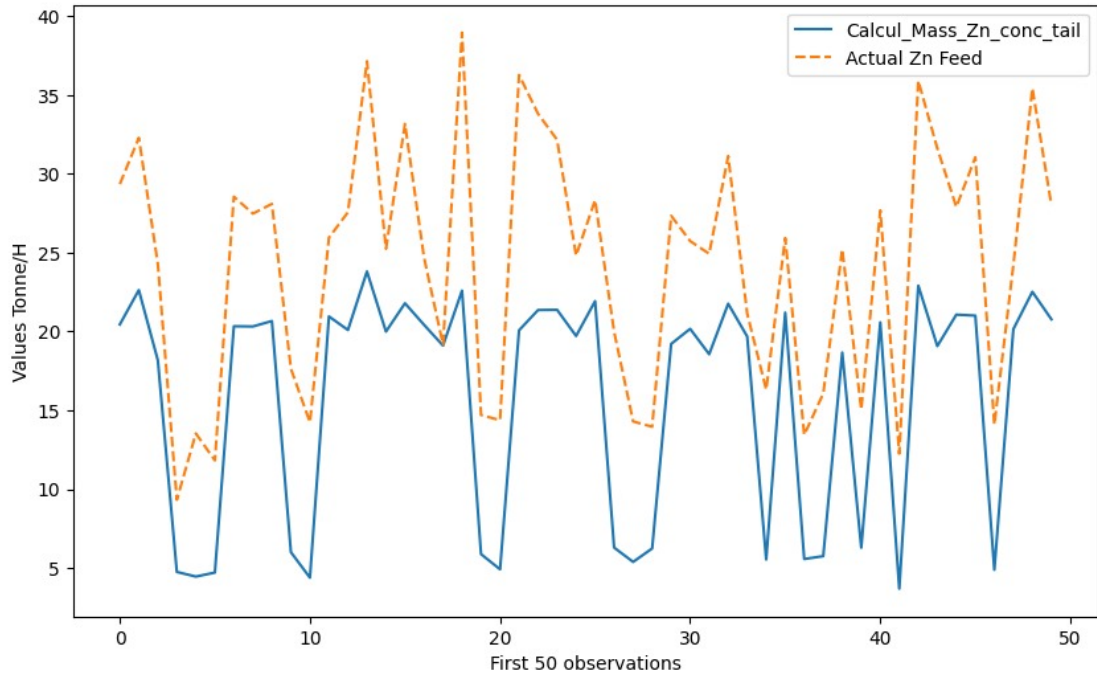


Figure 10: Predicted Zn feed VS Actual Zn feed

Description:

- **Calcul_Mass_Zn_conc_tail :**

shows fluctuations in its values throughout the 50 observations. This line has sharp increases and decreases, with the lowest points dipping just below 10 tonnes/H and the highest points reaching almost 40 tonnes/H.

- **Actual Zn Feed :**

which also shows fluctuations but with a general trend that seems to be increasing over the observed range. The values for this line also vary from just above 10 tonnes/H to nearly 40 tonnes/H.

The difference between the two curves appears to be in their volatility and the general trend. The **Calcul_Mass_Zn_conc_tail** line is more volatile with sharper peaks and troughs, while the **Actual Zn Feed** : line, although still fluctuating, seems to have a gentler wave pattern with a slight upward trend. It also appears that the "Actual Zn Feed" line has higher values on average compared to the **Calcul_Mass_Zn_conc_tail** line over the 50 observations.

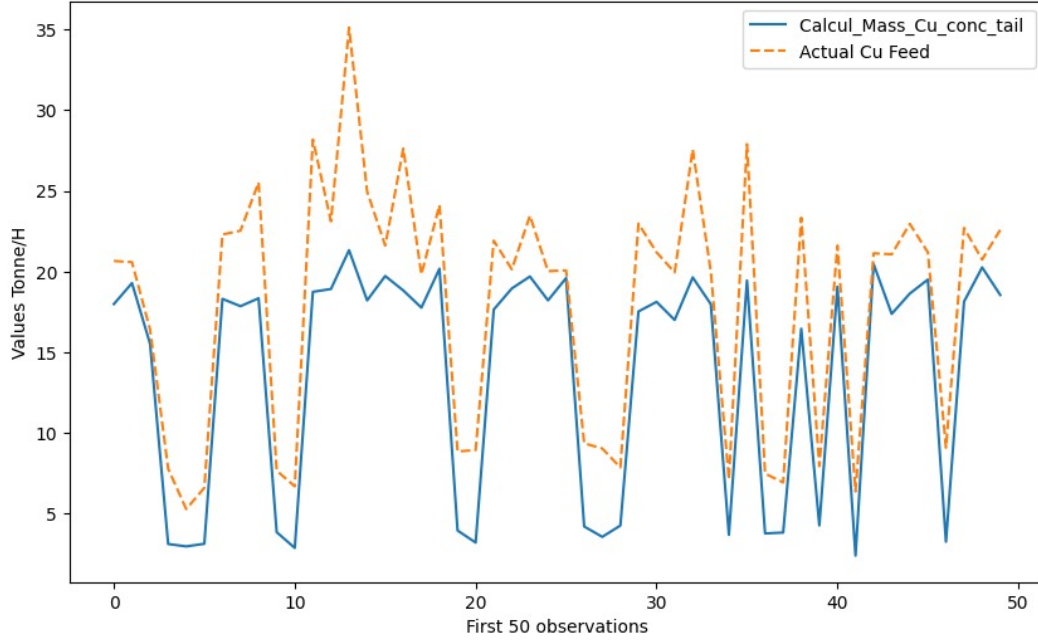


Figure 11: Predicted Cu feed VS Actual Cu feed

Description:

- Both lines show significant variability and some correlation, as they peak and dip around the same points, which indicates that the calculated values are somewhat reflective of the actual values. However, there are discrepancies where the dashed line (actual feed) peaks higher or dips lower than the solid line (calculated tailings), suggesting differences between the predicted and actual values.
- The overall message from the graph is that there's a good degree of correlation between the predicted and actual values, with some room for improvement in the prediction model.

5.4 Comparison with previous model's performance

This section provides a comparative analysis between the predictions of the Physics-Informed Neural Network (PINN) and those of a conventional Artificial Neural Network (ANN) specifically designed for the prediction of mineral concentrations. Visualizations showcase the side-by-side comparison of the two models, offering a

clear understanding of their respective performances. Through this comparative examination, insights are gained into the nuanced differences in their predictive capabilities, providing valuable information on the efficacy of the physics-informed regularization employed in the PINN architecture.

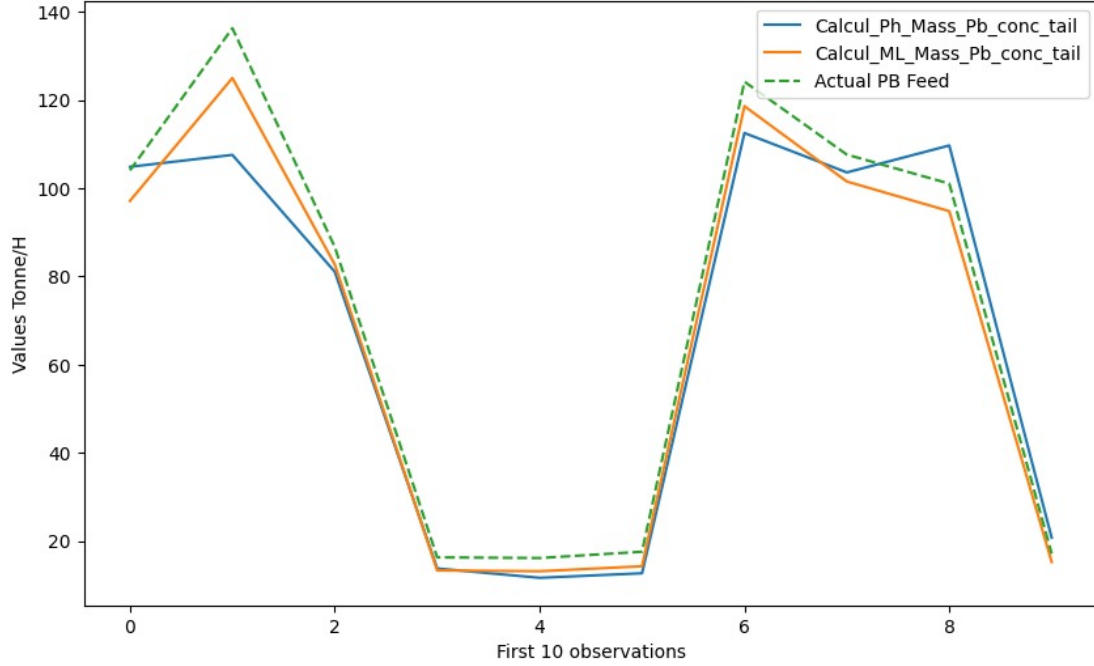


Figure 12: Actual PB VS ML's PB prediciton VS PINN's PB prediction

Description:

Calcul_Ph_Mass_Pb_conc_tail (solid light blue line): Starts at just above 100 tonnes/H, increases slightly, then decreases sharply to just below 60 tonnes/H, and then climbs steeply to just under 140 tonnes/H before decreasing again.

Calcul_ML_Mass_Pb_conc_tail (solid orange line): Begins just below the light blue line, follows the same initial increase and decrease, then ascends not quite as sharply, and finally falls in a similar fashion.

Actual PB Feed (dashed green line): This line starts just above 120 tonnes/H, decreases to around 60 tonnes/H, then rises sharply to the highest point of all lines at around 140 tonnes/H, and subsequently decreases.

All three lines show a similar pattern: a rise, followed by a sharp decline, then a step increase, and finally a drop off. The *Actual PB Feed* line shows the most significant increase, suggesting a higher feed rate compared to the calculated masses at around the 6th to 7th observation before the final decrease.

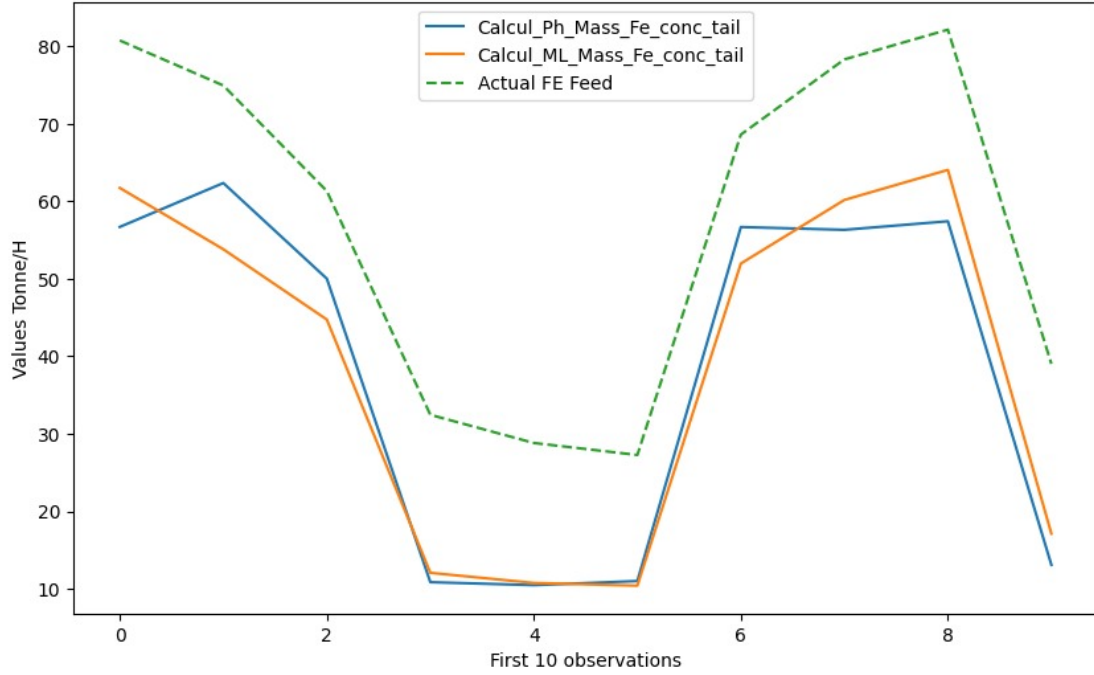


Figure 13: Actual Fe VS ML's Fe prediciton VS PINN's Fe prediction

Description:

Calcul_Ph_Mass_Fe_conc_tail (solid light blue line): Begins around 70 tonnes/H and decreases to around 30 tonnes/H by the 4th observation. It then increases sharply to over 70 tonnes/H by the 7th observation before dropping back down.

Calcul_ML_Mass_Fe_conc_tail (solid orange line): Starts slightly below the Calcul_Ph line, follows a similar downward trend, then rises less steeply than the Calcul_Ph line before falling again.

Actual FE Feed (dashed green line): Starts around 80 tonnes/H, decreases to below the other two lines by the 4th observation, then increases sharply, peaking above the others at around the 7th observation before falling.

All three lines decrease for the first half of the observations, then increase sharply around the 6th to 7th observation, with the Actual FE Feed showing the highest peak before decreasing again. The Actual FE Feed differs from the calculated masses, especially in the second half of the observations, where it peaks higher than both Calcul.Ph and Calcul.ML lines.

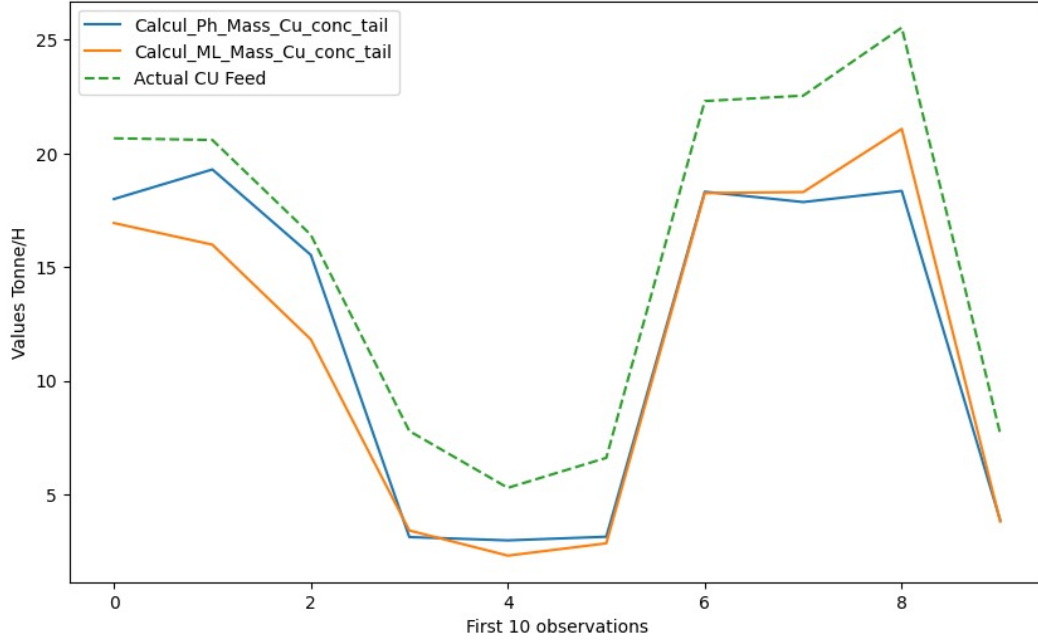


Figure 14: Actual Cu VS ML's Cu prediciton VS PINN's Cu prediction

Description:

Calcul_Ph_Mass_Cu_conc_tail (solid light blue line): This line starts just below 25 tonnes/H and generally decreases until the 6th observation before it rises sharply.

Calcul_ML_Mass_Cu_conc_tail (solid orange line): It starts slightly above the Calcul.Ph line and follows a similar downward trend until the 6th observation, then it increases but not as sharply as the Calcul.Ph line.

Actual CU Feed (dashed green line): This line starts just above 20 tonnes/H, decreases more steeply than the other two until the 6th observation, and then rises sharply, surpassing both Calcul.Ph and Calcul.ML lines before dropping again.

All three lines show a decrease followed by a sharp increase at the 6th observation. The Actual CU Feed line shows the most significant rise after the 6th observation, indicating a higher feed rate compared to the calculated masses. The three lines have similar trends, but the Actual CU Feed line differs noticeably in value, especially after the 6th observation.

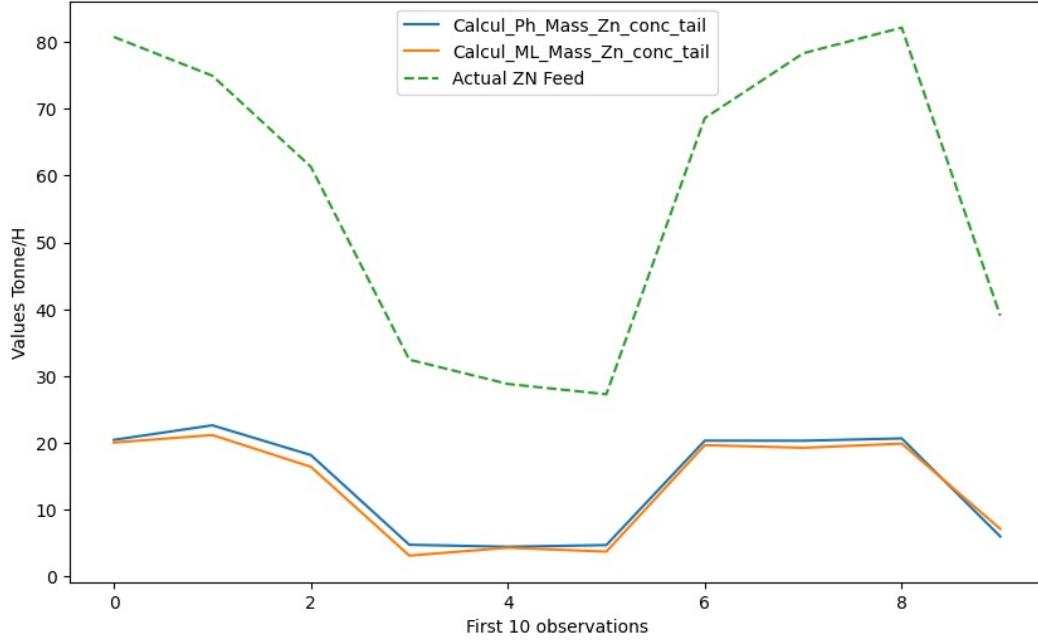


Figure 15: Actual Zn VS ML's Zn prediciton VS PINN's Zn prediction

Description:

Calcul_Ph_Mass_Zn_conc_tail (solid light blue line): This line has a relatively flat profile, with a gentle dip in the middle, starting and ending around 20 tonnes/H.

Calcul_ML_Mass_Zn_conc_tail (solid orange line): This line is nearly flat, with a very slight dip around the 4th observation, staying close to 20 tonnes/H throughout.

Actual ZN Feed (dashed green line): Starts at around 70 tonnes/H, decreases steeply to about 30 tonnes/H by the 4th observation, then increases sharply to about 80 tonnes/H by the 8th observation before the graph ends.

The *Actual ZN Feed* line is noticeably different from the *Calcul_Ph* and *Calcul_ML* lines. It shows a large variation in values, whereas the *Calcul_Ph* and *Calcul_ML* lines remain relatively consistent and much closer to each other throughout the 10 observations.

6 Conclusion

This report has presented a comprehensive investigation into the application of a Physics-Informed Neural Network (PINN) for the prediction of mineral concentrations. By integrating physics-driven constraints, the PINN demonstrates its capacity to not only provide accurate predictions but also ensure adherence to fundamental mass conservation laws.

The visual comparisons between PINN predictions and observed values underscore the model's ability to capture the complexities of mineral compositions. Furthermore, the comparative analysis with a conventional Artificial Neural Network (ANN) illuminates the added value of incorporating physics-informed regularization, showcasing the PINN's superior performance in accurately predicting mineral concentrations.

The study not only contributes to the advancement of predictive modeling in mineral processing but also highlights the potential for physics-informed approaches to enhance the reliability and interpretability of machine learning models in complex systems.